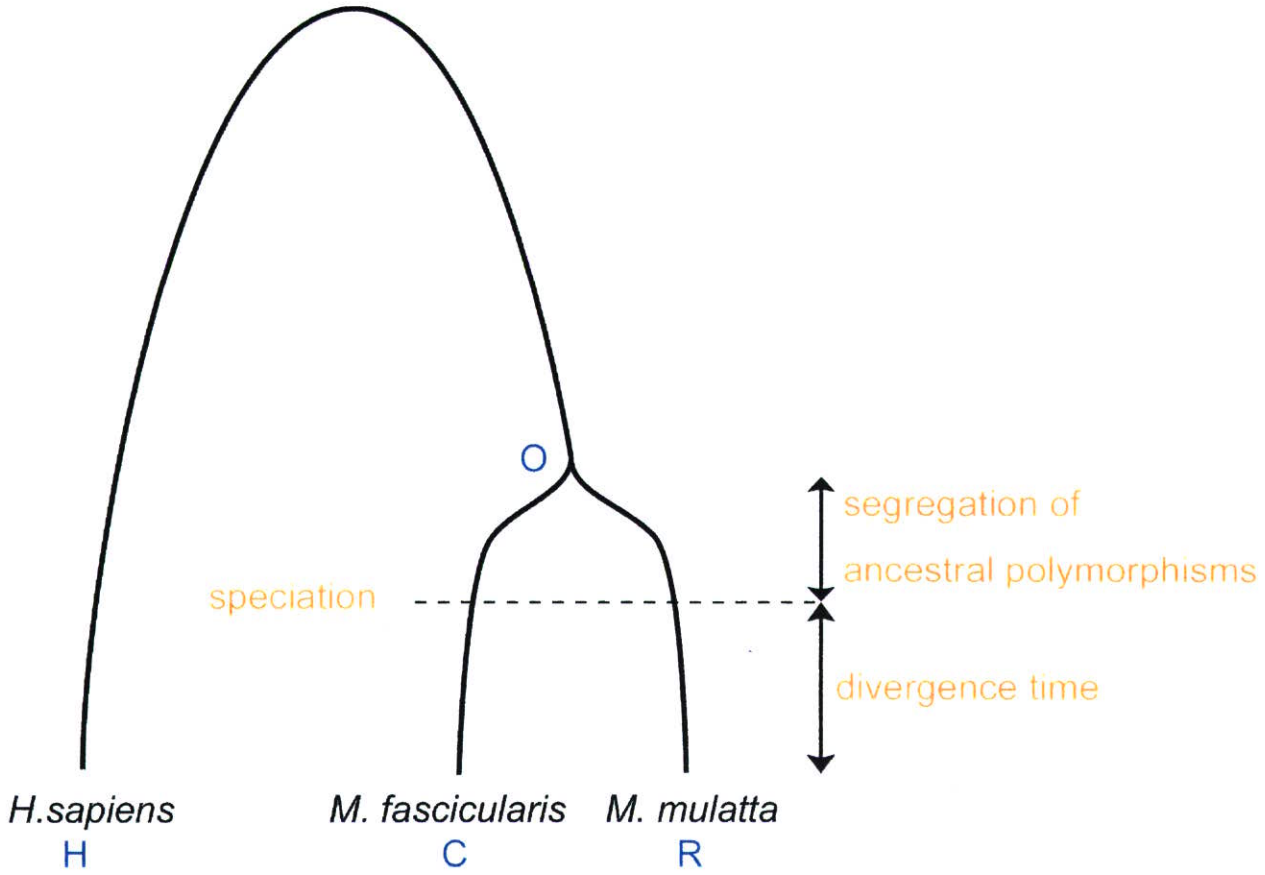
O
segregation of
ancestral polymorphisms
speciation
divergence time
H.sapiens
H
M. fascicularis
C
M. mulatta
R

Additional files provided with this submission:

Additional file 1: supplementarytable1.xls, 1247K
http://www.biomedcentral.com/imedia/1968231173184153/supp1.xls
Additional file 2: supplementarytable2.xls, 287K
http://www.biomedcentral.com/imedia/1209966074184154/supp2.xls
Additional file 3: supplementarytable3.doc, 35K
http://www.biomedcentral.com/imedia/1259421256184154/supp3.doc
Additional file 4: supplementarytable4.xls, 29K
http://www.biomedcentral.com/imedia/4376573111841540/supp4.xls
Additional file 5: supplementarytable5.xls, 57K
http://www.biomedcentral.com/imedia/1946285321184154/supp5.xls
Additional file 6: supplementarytable6.xls, 17K
http://www.biomedcentral.com/imedia/1343814754184154/supp6.xls

nature
cell biology

The lipid droplet is an important organelle for hepatitis C virus production

Yusuke Miyanari[1,2], Kimie Atsuzawa[3], Nobuteru Usuda[3], Koichi Watashi[1,2], Takayuki Hishiki[1,2], Margarita Zayas[4], Ralf Bartenschlager[4], Takaji Wakita[5], Makoto Hijikata[1,2] and Kunitada Shimotohno[1,2,6]

The lipid droplet (LD) is an organelle that is used for the storage of neutral lipids. It dynamically moves through the cytoplasm, interacting with other organelles, including the endoplasmic reticulum (ER)[1–3]. These interactions are thought to facilitate the transport of lipids and proteins to other organelles. The hepatitis C virus (HCV) is a causative agent of chronic liver diseases[4]. HCV capsid protein (Core) associates with the LD[5], envelope proteins E1 and E2 reside in the ER lumen[6], and the viral replicase is assumed to localize on ER-derived membranes. How and where HCV particles are assembled, however, is poorly understood. Here, we show that the LD is involved in the production of infectious virus particles. We demonstrate that Core recruits nonstructural (NS) proteins and replication complexes to LD-associated membranes, and that this recruitment is critical for producing infectious viruses. Furthermore, virus particles were observed in close proximity to LDs, indicating that some steps of virus assembly take place around LDs. This study reveals a novel function of LDs in the assembly of infectious HCV and provides a new perspective on how viruses usurp cellular functions.

Hepatitis C virus (HCV) has a plus-strand RNA genome that encodes the viral structural proteins Core, E1 and E2, the p7, and the nonstructural (NS) proteins 2, 3, 4A, 4B, 5A and 5B (refs 7, 8). NS proteins are reported to localize on the cytoplasmic side of endoplasmic reticulum (ER) membranes[9]. To elucidate the mechanisms of virus production, we used a HCV strain, JFH1, which can produce infectious viruses[10–12]. We first investigated the subcellular localization of the HCV proteins in cells that had been transfected with JFH1^{E2FL} RNA, in which a part of the hypervariable region 1 of E2 was replaced by the FLAG epitope tag (see Supplementary Information, Fig. S1, S2a–d). Core localized to the lipid droplets (LDs; Fig. 1a), as previously reported[5]. Interestingly, NS proteins were also detected around LDs in 60–90% of JFH1^{E2FL}-replicating cells (Fig. 1a, c). Similar levels of colocalization of LDs with viral proteins were observed in cells that had been transfected with chimeric HCV genomes expressing structural proteins, p7 and part of NS2 of the genotype 1b (Con1) or the genotype 1a (H77) isolate (see Supplementary Information, Fig. S1, S2e)[13]. In contrast, there was no close association between the LDs and NS proteins in cells that had been transfected with JFH1^{dC3} RNA (Fig. 1b, c), which lacked the coding region of Core (Supplementary Information, Fig. S1). NS proteins were diffusely present on the ER, suggesting that NS proteins are translocated from the ER to LDs in JFH1^{E2FL}-replicating cells in a Core-dependent manner. Importantly, there was no association between LDs and PDI, an ER marker protein, indicating that either ER membranes were absent in close proximity to LDs or that PDI was excluded from such membranes (Fig. 1c). These results were supported by western blot analysis of the LD fraction (Fig. 1d). The LD fraction contained ADRP, an LD marker, but not the ER markers Calnexin and Grp78 (data not shown), indicating that there was no ER contamination in the LD fraction. However, the LD fraction from JFH1^{E2FL}-replicating cells contained high levels of viral proteins in contrast to the LD fraction from JFH1^{dC3}-replicating cells (in which HCV proteins were virtually absent (Fig. 1d, LD fraction)), even though the expression levels of the NS proteins in whole-cell extracts were similar (Fig. 1d, whole-cell extract). About 20–45% of the total HCV proteins associated with the LDs in JFH1^{E2FL}-replicating cells (Fig. 1e). Consistent with previous reports that Core enhances the formation of LDs[14], overproduction of LDs was observed in JFH1^{E2FL}-, but not JFH1^{dC3}-replicating cells (Supplementary Information, Fig. S3a–l). Treatment of the cells with oleic acid, which enhanced the formation of LDs, did not affect either HCV protein levels or the recruitment of viral proteins to LDs in JFH1^{dC3}-replicating cells (Supplementary Information, Fig. S3m–p). Thus, the overproduction of LDs is insufficient for the recruitment of HCV proteins to LDs. To examine the ability of Core to recruit NS proteins to LDs, JFH1^{dC3}-replicating cells were transfected with a plasmid-expressing Core (Core^{WT}) (Fig. 1f, g). NS5A accumulated around LDs (Fig. 1f, arrowheads and panel 2), as did NS3 and NS4AB (Fig. 1g), in cells expressing Core^{WT}. The translocation of NS proteins to LDs was, however, not observed in JFH1^{dC3}-replicating cells expressing Core$^{PP/AA}$ (Fig. 1g and Supplementary Information, Fig. S2f–h),

[1]Department of Viral Oncology, Institute for Virus Research, Kyoto University, Kyoto 606-8507, Japan; [2]Graduate School of Biostudies, Kyoto University, Kyoto 606-8507, Japan; [3]Department of Anatomy, Fujita Health University School of Medicine, Toyoake 470-1192, Japan; [4]Department of Molecular Virology, University of Heidelberg, 69120 Heidelberg, Germany; [5]Department of Virology II, National Institute of Infectious Diseases, Tokyo 162-8640, Japan
[6]Correspondence should be addressed to K.S. (e-mail: shimkuni@z8.keio.jp)

Received 16 March 2007; accepted 31 July 2007; published online 26 August 2007; DOI: 10.1038/ncb1631

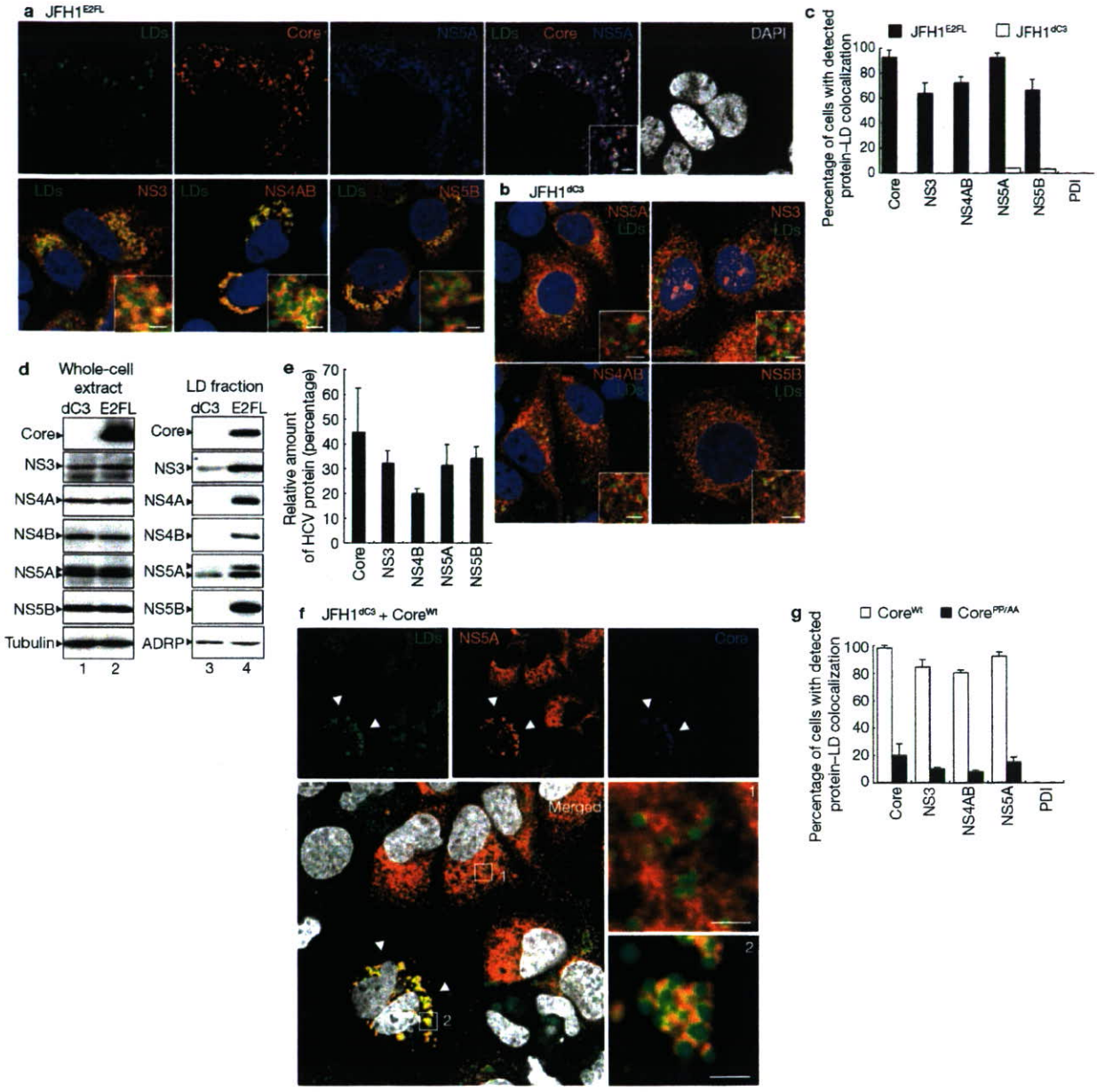

Figure 1 Core recruits NS proteins to LDs. **(a)** Huh-7 cells transfected with JFH1^{E2FL} RNA were labelled with antibodies against Core (red), NS5A (blue), NS3 (red), NS4AB (red) or NS5B (red). Lipid droplets (LDs) and nuclei were stained with BODYPI 493/503 (green) and DAPI (white in upper panel, blue in lower panels), respectively. Insets are high magnification images of areas in the respective panel. **(b)** JFH1^{dC3} replicon-bearing cells were labelled with DAPI (blue), BODIPY 493/503 (green) and indicated antibodies (red). The insets are high magnifications of the corresponding panel. **(c)** Percentages of JFH1^{E2FL}- or JFH1^{dC3}-bearing cells in which hepatitis C virus (HCV) proteins or PDI colocalize with LDs ($n > 200$). **(d)** Western blot analysis of HCV proteins and marker proteins in whole-cell extracts and the LD fractions from cells transfected with JFH1^{E2FL} (E2FL) or JFH1^{dC3} (dC3) RNA. **(e)** HCV proteins were quantified by using western blotting data of the purified LD fraction and whole-cell extracts of JFH1^{E2FL}-replicating cells. Results are shown as relative amounts of HCV proteins co-fractionated with LDs. This results correspond well with results obtained by quantitative immunofluorescence staining (data not shown). **(f)** Trans-complementation with Core^{Wt} relocates NS proteins to LDs. JFH1^{dC3} replicon-bearing cells were transfected with pcDNA3–Core^{Wt} and labelled with BODIPY 493/503 (green), DAPI (white) and antibodies against NS5A (red) and Core (blue). Arrowheads indicate Core^{Wt}-expressing cells. Higher-magnification images of area 1 and area 2 are shown in panels 1 and 2, respectively. Scale bars, 2 μm. **(g)** The percentages of cells in which HCV proteins colocalize with LDs in the presence of Core^{Wt} or Core $^{PP/AA}$ ($n > 200$). Uncropped images of gels are shown in Supplementary Information Fig. S6. All error bars are derived from s.d.

a variant of Core containing two alanine substitutions at amino-acid positions 138 and 143 that fails to associate with LDs[15]. These results show that LD-associated Core recruits NS proteins from the ER to LDs.

Next, we investigated whether Core also recruited HCV RNA to LDs. *In situ* hybridization analysis showed that in more than 80% of JFH1^{E2FL}-replicating cells, both plus- and minus-strand RNAs were diffusely

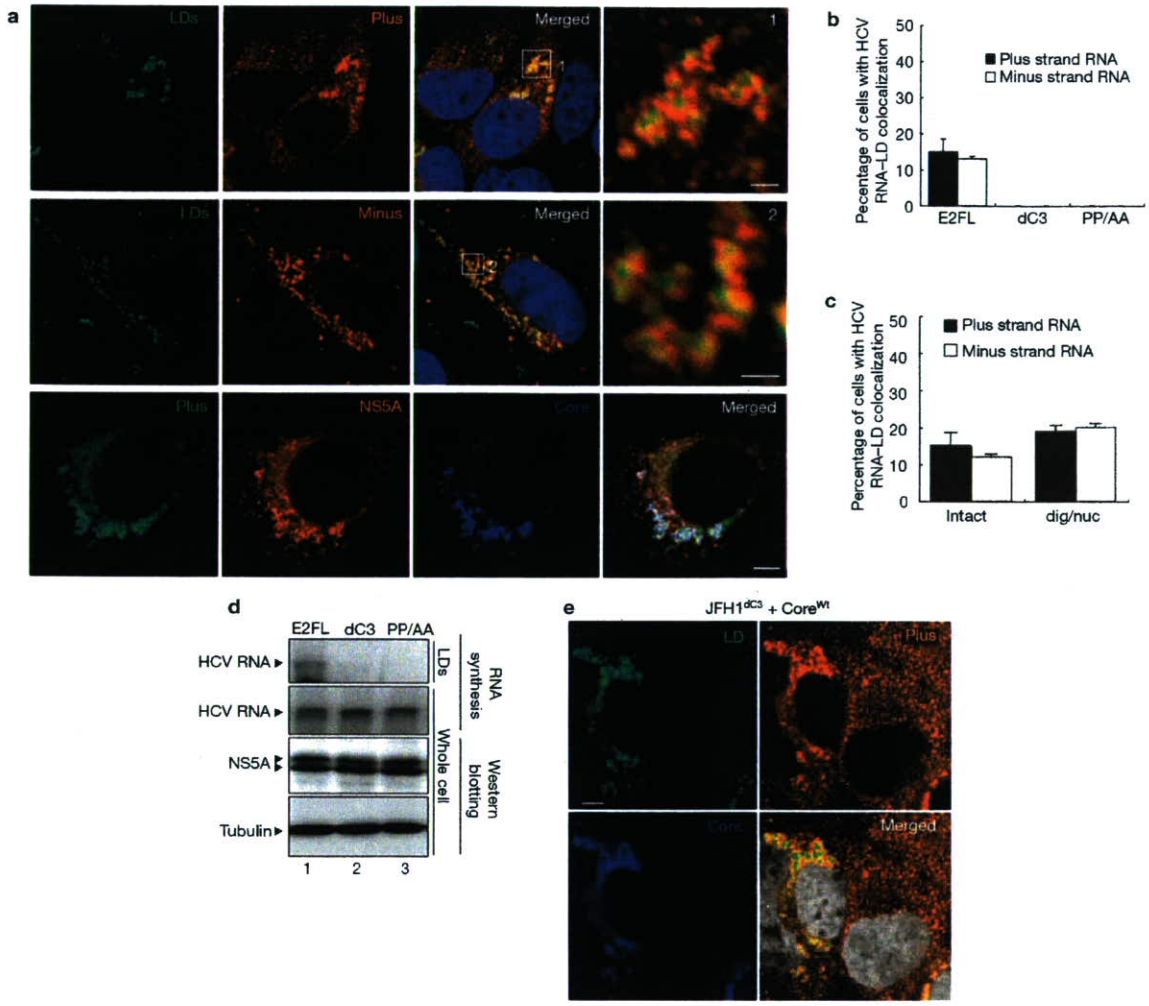

Figure 2 Core-dependent recruitment of active HCV replication complexes to the LD. (**a**) Huh-7 cells transfected with JFH1^{E2FL} RNA were analysed by *in situ* hybridization with strand-specific probes (plus or minus). The cells were labelled to simultaneously visualize lipid droplets (LDs), NS5A and Core (lower panels). Higher-magnification images of area 1 and area 2 are shown in the upper and middle right panels 1 and 2, respectively. Scale bars: 2 μm (panels 1, 2); 10 μm (lower right panel). (**b**) The percentages of JFH1^{E2FL}-, JFH1^{dC3}- and JFH1$^{PP/AA}$-expressing cells positive for overlapping signals for LDs and plus- or minus-strand hepatitis C virus (HCV) RNA ($n > 200$). (**c**) Intact or digitonin and nuclease-treated (dig/nuc) JFH1^{E2FL} replicon-bearing cells were analysed by *in situ* hybridization. The percentages of cells with overlapping signals for LD and plus- or minus-strand HCV RNA are shown ($n > 200$). (**d**) RNA-synthesizing activity in the LD fractions purified from cells transfected with JFH1^{E2FL}, JFH1^{dC3} or JFH1$^{PP/AA}$ RNA (top panel). As a control, HCV RNA synthesis activity in digitonin-permeabilized cells was analysed (second panel from the top). HCV protein levels represented by NS5A are shown, together with the level of tubulin (bottom two panels). (**e**) Localization of plus-strand HCV RNA and Core in JFH1^{dC3} replicon-bearing cells transfected with pcDNA3–Core^{Wt} (Scale bar, 10 μm). Uncropped images of gels are shown in Supplementary Information Fig. S6. All error bars are derived from s.d.

located in the perinuclear region (see Supplementary Information, Fig. S4a). More importantly, in about 20% of these cells, plus- and minus-strand RNAs accumulated around LDs (Fig. 2a, upper and middle panels; 2b) and colocalized with HCV proteins such as Core and NS5A (Fig. 2a, lower panels). No association between HCV RNA and LDs was detected in JFH1^{dC3}- or JFH1$^{PP/AA}$-replicating cells (Fig. 2b). Northern blot analysis revealed that 4.8% and 5.4% of total plus- and minus-strand HCV RNA, respectively, were detected in purified LD fractions of JFH^{E2FL}-replicating cells (data not shown). Induction of LD formation with oleic acid did not affect HCV RNA accumulation around LDs (data not shown). These results provide strong evidence that Core recruits HCV RNA as well as NS proteins to LDs.

The HCV replication complex is compartmentalized by lipid bilayer membranes[16–18]. Therefore, HCV RNA in the complex is resistant to nuclease treatment in digitonin-permeabilized cells[17] (Supplementary Information, Fig. S4b–d). *In situ* hybridization analysis did not reveal a significant difference in the number of cells containing LD-associated HCV RNA before and after nuclease treatment (Fig. 2c), indicating that HCV RNA around LDs is part of the replication complex. An RNA synthesis assay showed that the purified LD fraction from JFH1^{E2FL}-, but not JFH1^{dC3}- or JFH1$^{PP/AA}$-replicating cells, possessed HCV RNA synthesis activity, even though the expression levels of viral proteins and RNA-synthesizing activities in total cell lysates were similar (Fig. 2d). Moreover, the addition of Core^{Wt} rescued the localization of plus- and minus-strand

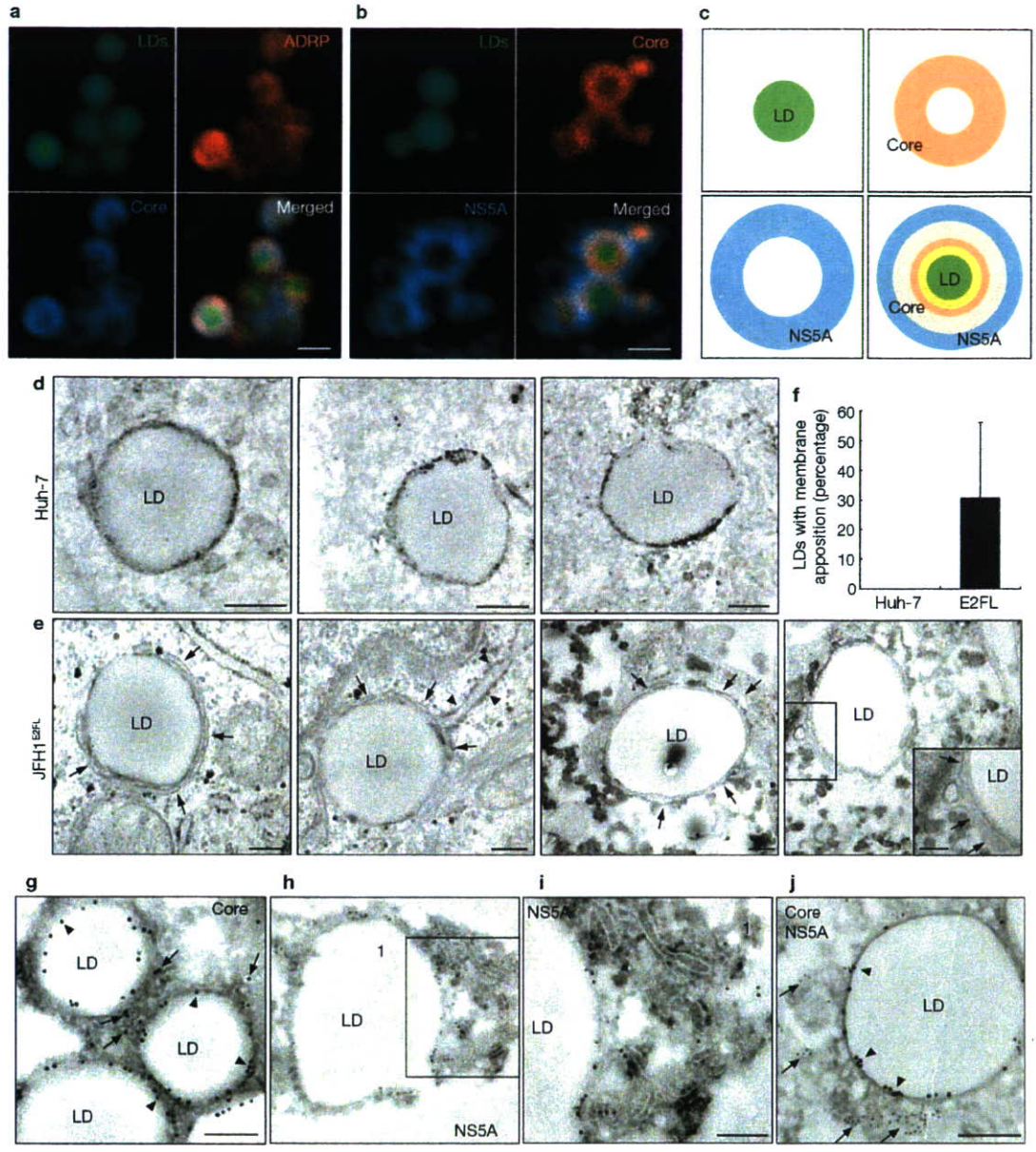

Figure 3 Spatial distribution of Core and NS5A relative to the LD. (**a**, **b**) The localizations of Core, NS5A and ADRP around the lipid droplets (LDs) in JFH1^{E2FL} replicon-bearing cells were analysed using immunofluorescence microscopy. Scale bars, 1 μm. (**c**) Typical images of the localization of LDs, Core, NS5A and merged images are shown with the relative scale of each image. (**d**, **e**) Transmission electron micrographs of LDs in naïve Huh-7 cells and JFH1^{E2FL}-expressing cells. Arrows and arrowheads indicate LD-associated membranes and rough ER membranes, respectively. (**f**) Frequency of LDs with close appositions of membrane cisternae. About 100 Huh-7 cells or JFH1^{E2FL}-expressing cells, respectively, were chosen randomly. LDs with apposed membrane cisternae, as exemplified in panel **e**, were counted as positive. The LDs judged as positive were divided by the total number of LDs. (**g**–**j**) Immunoelectron micrographs of LDs labelled with antibodies against Core (**g**), NS5A (**h**, **i**) or both (**j**) are shown. Panel **i** is a higher magnification of area 1 in panel **h**. In panel **j**, Core and NS5A are labelled with 15 nm and 10 nm gold particles, respectively. Scale bars, 200 nm. All error bars are derived from s.d.

HCV RNA around LDs in JFH^{dC3}-replicating cells (Fig. 2e and data not shown). Both plus- and minus-strand RNA associated with LDs were nuclease resistant (data not shown). These results demonstrate that Core recruits biologically active replication complexes to LDs.

The LD is surrounded by a phospholipid monolayer[19], whereas HCV replication complexes are likely to be surrounded by lipid bilayer membranes[16,17]. Therefore, the replication complexes might not be directly associated with the membranes of LDs. To characterize the colocalization of LDs, viral proteins and replication complexes more precisely, we analysed the localization of NS5A with high-resolution immunofluorescence microscopy. Core was completely colocalized with ADRP, residing on the surface of LDs[20] (Fig. 3a), thus indicating that Core also directly associates with the surface of LDs. More importantly, NS5A mainly localized around the Core-positive area, resulting in a doughnut-shaped signal with a diameter slightly

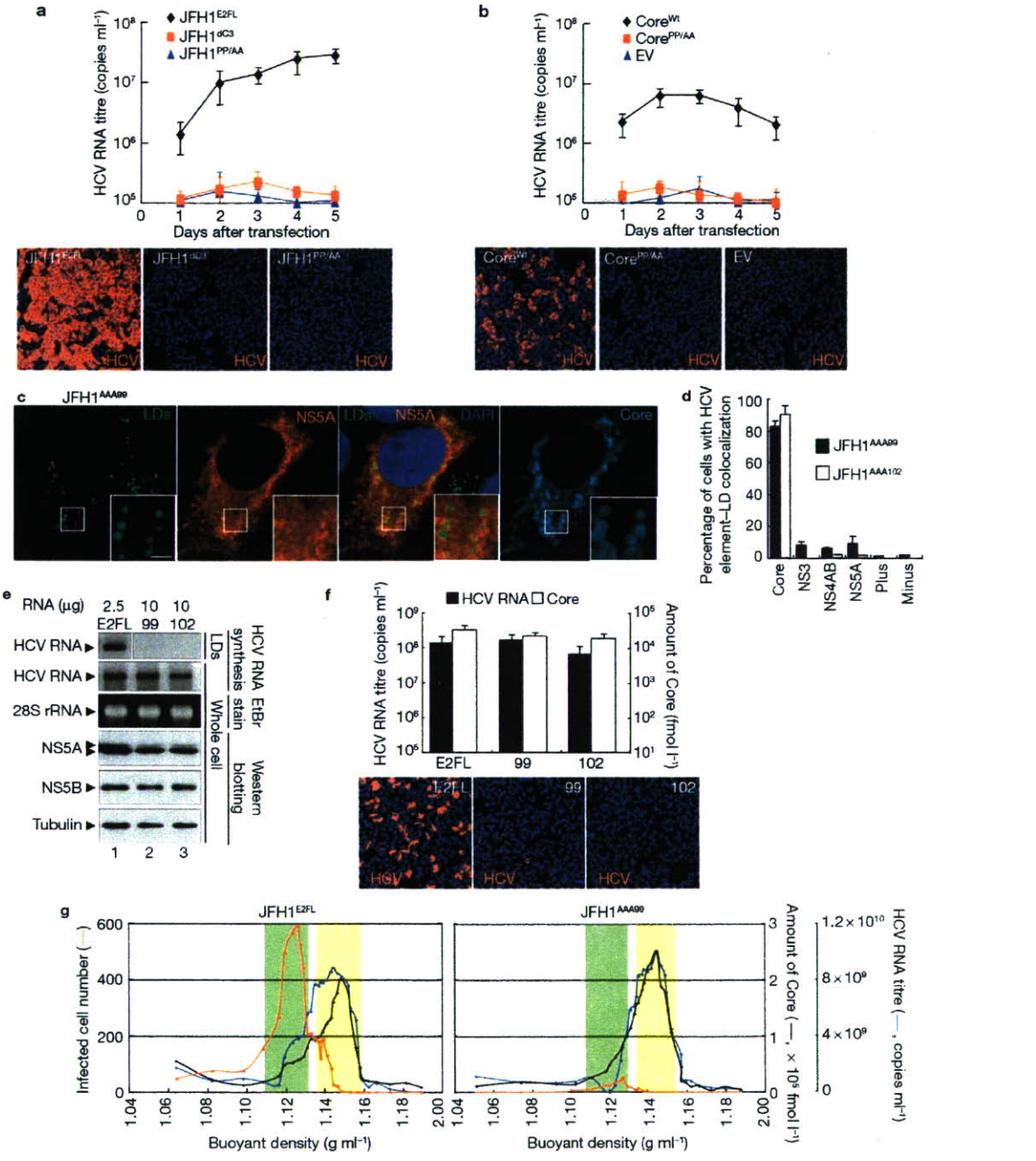

Figure 4 LD associations of Core and NS proteins are necessary for the production of infectious HCV particles. (**a**) The culture medium from JFH1^{E2FL}-, JFH1^{dC3}- or JFH1$^{PP/AA}$-replicating cells was collected at the indicated time points and the titre of hepatitis C virus (HCV) RNA was measured by real-time RT-PCR (upper panel, $n = 3$). The culture medium was added to naïve Huh7.5 cells and, 24 h after inoculation, and cells were labelled with anti-HCV antibodies (lower panels, red). (**b**) JFH1^{dC3} replicon-bearing cells were transfected with pcDNA3 (EV), pcDNA3–Core^{Wt} (Core^{Wt}) or pcDNA3–Core$^{PP/AA}$ (Core$^{PP/AA}$). The level of HCV RNA and the infectivity of the culture medium were examined as described above ($n = 3$). (**c**) Subcellular localization of NS5A and Core in cells expressing JFH1^{AAA99}. The insets are high magnifications of the area of the corresponding panel. Scale bar, 2 μm. (**d**) Percentages of cells in which the signals for given HCV proteins, and plus- and minus-strand HCV RNA, overlapped with those for LDs ($n > 200$). (**e**) Different amounts of JFH1^{E2FL} (E2FL), JFH1^{AAA99} (99) or JFH1^{AAA102} (102) RNAs, respectively, were transfected into the same number of Huh-7 cells. HCV RNA synthesis activity in purified LD fractions (LD) and whole-cell lysates (whole cell) was analysed (HCV RNA synthesis). 28S rRNA was used as a control. Western blot analysis of NS5A, NS5B and tubulin in cells is also shown. All the RNA samples in the top panel were run on the same gel. (**f**) Analysis of HCV released from cells expressing JFH1^{E2FL}, JFH1^{AAA99} or JFH1^{AAA102}. HCV RNA titres (black bars) and amounts of Core (white bars) accumulated in the culture medium at 5 d after RNA transfection were measured (upper panel, $n = 3$). Infectivity of the culture medium for naïve Huh-7.5 cells was analysed as described above (lower panels). (**g**) Concentrated culture medium from JFH1^{E2FL}- and JFH1^{AAA99}-replicating cells was fractionated using 20–50% sucrose density-gradient centrifugation at 100,000 *g* for 16 h. For each fraction, the amounts of Core (black line), HCV RNA (blue line) and infectivity (represented by infected cell numbers in a well; red line) are plotted against the buoyant density (*x*-axis) ($n = 3$). Uncropped images of gels are shown in Supplementary Information Fig. S6. All error bars are derived from s.d.

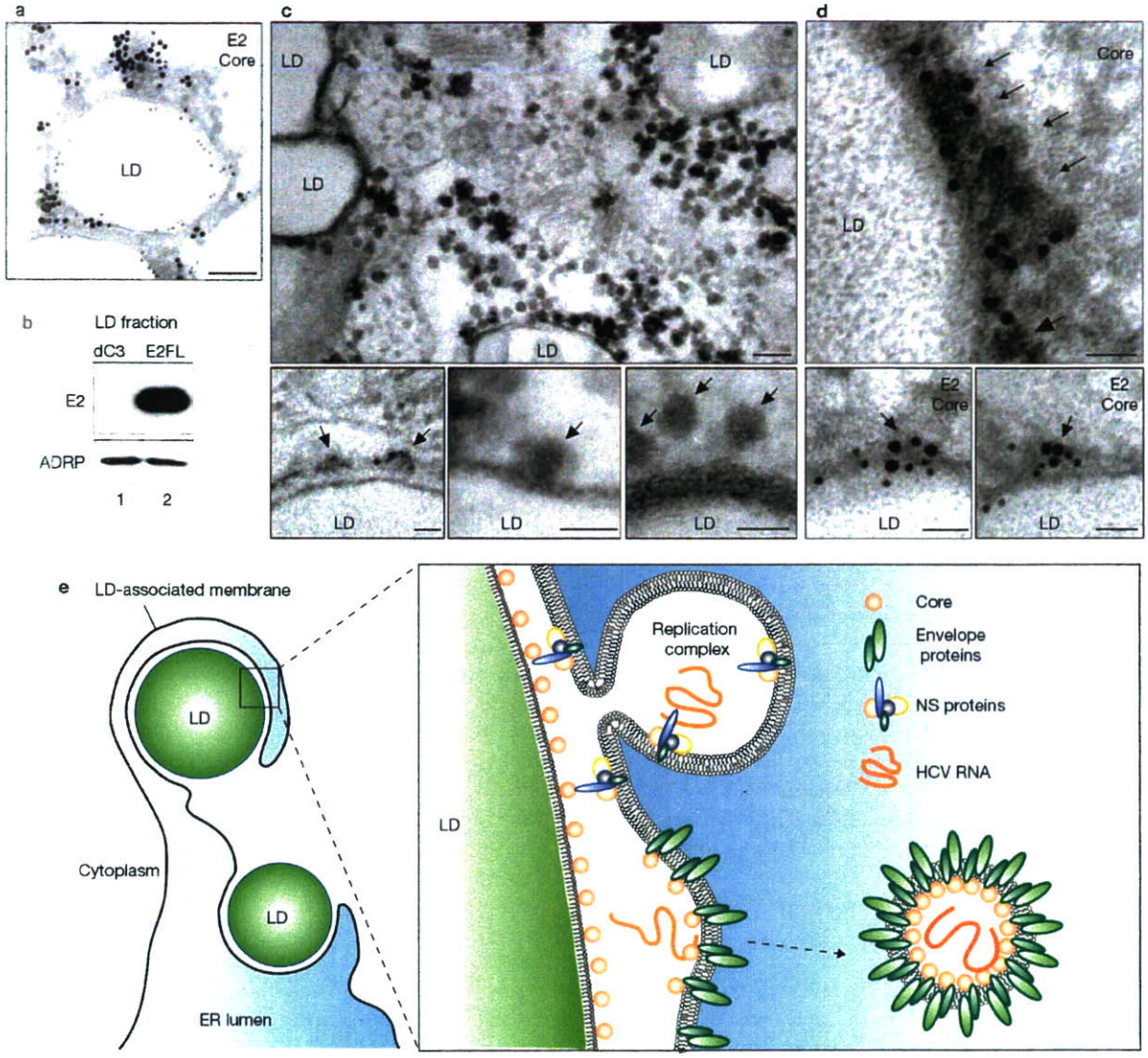

Figure 5 Virus-assembly takes place around the LDs. (**a**) Immunoelectron microscopic detection of E2 and Core in JFH1^{E2FL}-replicating cells. E2 and Core are labelled with 15 nm and 10 nm gold particles, respectively. (**b**) Western blot analysis of the lipid droplet (LD) fraction from JFH1^{E2FL} and JFH1^{dC3} replicon-bearing cells with anti-E2 and anti-ADRP antibodies. (**c**) Transmission electron micrographs of JFH1^{E2FL}-replicating cells. Arrows indicate virus-like particles. (**d**) Immunoelectron micrographs of LDs labelled with antibodies against Core (10 nm) and E2 (15 nm) are shown. Arrows show Core in electron-dense granules. Scale bar: **a** and upper panel of **c**: 100 nm; in **d** and lower panels of **c**: 50 nm. (**e**) A model for the production of infectious hepatitis C virus (HCV). Core mainly localizes on the monolayer membrane that surrounds the LD. HCV induces the apposition of the LD to the endoplasmic reticulum (ER)-derived bilayer membranes (LD-associated membrane). Core recruits NS proteins, as well as replication complexes, to the LD-associated membrane. NS proteins around the LD can then participate in infectious virus production. E2 also localizes around the LD. Through these associations, virion assembly proceeds in this local environment. Uncropped images of gels are shown in Supplementary Information Fig. S6.

larger than that of Core (Fig. 3b). The LD-proximal NS5A signal partially overlapped with the Core signal (Fig. 3b, c, grey). This concentric staining pattern was also observed with the other NS proteins (Supplementary Information, Fig. S5a), indicating that NS proteins associate with Core on the surface of LDs. Electron microscopic analysis only rarely revealed a close association of LDs with other organelles in naïve Huh-7 cells (Fig. 3d, f). However, in the case of JFH1^{E2FL}-replicating cells, about 30% of the LDs were in close proximity to membrane cisternae (Fig. 3e, arrows; 3f), arguing for a HCV-induced membrane rearrangement around LDs. Core was mainly located on the periphery of LDs, and occasionally signals were observed in more distal areas of the LDs (Fig. 3g, arrowheads and arrows, respectively). Although some NS5A signals were observed on the surface of the LD, the majority of NS5A signals were detected more distal of LDs (Fig. 3h, i). Furthermore, we often observed membrane cisternae as white lines in the same area as NS5A signals (Fig. 3i, arrows). When the same section was labelled with anti-Core and anti-NS5A antibodies, Core was detected on the surface of the LDs, whereas NS5A was mainly observed in the peripheral area of the LDs (Fig. 3j, arrowheads and arrows, respectively). In summary, these results show that Core recruits NS proteins, as well as HCV replication complexes, to the LD-associated membranes.

The above results prompted us to ask whether Core–LD colocalization is important for the production of infectious virus particles. JFH1^{E2FL}-replicating cells released virions into the culture medium and these viruses were highly infectious for naïve Huh-7.5 cells[11,21], although culture medium from JFH1$^{PP/AA}$- or JFH1^{dC3}-replicating cells did not contain significant levels of HCV RNA and infectious virus (Fig. 4a). However, following trans-complementation with Core^{Wt}, a high titre of HCV RNA and infectious virus could be rescued from JFH1^{dC3}-replicating cells (Fig. 4b; and see Supplementary Information, Fig. S5b, c). In contrast, the production of infectious viruses was not rescued by trans-complementation with Core$^{PP/AA}$ (Fig. 4b). RNA-binding properties and oligomerization of Core^{Wt} and Core$^{PP/AA}$, which are both necessary for virus assembly, were similar (Supplementary Information, Fig. S5d; ref. 22), arguing that the primary defect of this mutant in preventing infectious virus production is the inability to associate with LDs.

To investigate the contribution of NS proteins around LDs to infectious virus production, we used variants of NS5A, which were not recruited to LDs even in the presence of Core. We assumed that NS5A was crucial for recruiting other NS proteins to LDs, because the level of NS5A recruited to LDs via Core was higher than the levels of the other recruited NS proteins (Fig. 1c, JFH1^{E2FL}). Using alanine-scanning mutagenesis within the NS5A coding region of JFH1^{E2FL}, we generated two mutants, JFH1^{AAA99} and JFH1^{AAA102}, in which the amino-acid sequence APK (aa 99–101 of NS5A) or PPT (aa 102–104 of NS5A) was replaced by AAA (Supplementary Information, Fig. S1). In JFH1^{AAA99}- and JFH1^{AAA102}-replicating cells, NS5A was rarely detected around LDs, whereas Core was still localized to LDs (Fig. 4c, d). Importantly, these mutations impaired not only the NS5A association with LDs, but also the recruitment of other NS proteins and viral RNAs to LDs (Fig. 4d). These results indicate that NS5A is a key protein that recruits replication complexes to LDs. Importantly, HCV RNA synthesis activity in the LD fractions from these mutant JFH1-replicating cells was also severely impaired (Fig. 4e), corroborating the lack of association of HCV replication complexes with LDs.

To investigate the infectious virus production of these NS5A mutants, we prepared cells expressing similar levels of HCV proteins and RNA by adjusting the amount of transfected HCV RNA (Fig. 4e). This was necessary, because replication activities of these mutants were lower compared with JFH1^{E2FL}. Under these conditions, the amounts of Core and HCV RNA that were released into the culture medium from cells transfected with the mutants were comparable to JFH ^{E2FL} (Fig. 4f, upper graph). However, infectivity titres of the mutants were severely reduced (Fig. 4f, lower panels). In sucrose density-gradient centrifugation of culture medium from JFH1^{E2FL}-bearing cells, two types of HCV particles were detected: low-density particles (about 1.12 g ml^{-1}) with high infectivity (Fig. 4g, green area of JFH1^{E2FL}), and high-density particles (about 1.15 g ml^{-1}) without infectivity (yellow area). This result indicates that only a minor portion of released HCV particles is infectious, whereas the majority of released particles lack infectivity. In contrast, cells bearing the JFH1^{AAA99} mutant almost exclusively released non-infectious particles of around 1.15 g ml^{-1}, whereas infectious particles were barely detectable (Fig. 4g, JFH1^{AAA99}). Taken together, these results provide convincing evidence that the association of NS proteins and replication complexes around LDs is critical for producing infectious viruses, whereas production of non-infectious viruses seems to follow a different pathway.

The results described so far imply that some step(s) of HCV assembly take place around LDs. To explore this possibility, we analysed the distribution of the major envelope protein E2 around the LD. Electron microscopic analysis revealed that, in about 90% of JFH1^{E2FL}-replicating cells, E2 was localized in the peripheral area of the LDs (Fig. 5a, large grains). This labelling pattern was similar to the one observed for NS5A (Fig. 3j), indicating that E2 also localizes on the LD-associated membranes. Western blot analysis of the LD fraction supported this conclusion, because the LD fraction that was purified from JFH1^{E2FL}-replicating cells, but not from JFH1^{dC3}-replicating cells, contained E2 (Fig. 5b). Furthermore, spherical virus-like particles with an average diameter of about 50 nm were observed around LDs in JFH1^{E2FL}-replicating cells (Fig. 5c, upper panel). These particles were never observed in naïve Huh-7 cells. A more refined analysis indicates that these particles are closely associated with membranes in close proximity to LDs (Fig. 5c, lower panels, arrows). Finally, these particles around the LDs reacted with Core- and E2-specific antibodies, arguing that the particles represent true HCV virions (Fig. 5d). These results suggest that infectious HCV particles are generated from the LD-associated membranous environment.

In this study, we have demonstrated that Core recruits NS proteins, HCV RNAs and the replication complex to LD-associated membranes. Mutations of Core and NS5A (Fig. 4), which failed to associate with LDs, impaired the production of infectious virus. We note that the mutant Core retains the ability to interact with RNA (Supplementary Information, Fig. S5b) and to assemble into nucleocapside[22]. Similarly, the NS5A mutant still supports viral genome replication and the formation of capsids or virus-like particles, arguing that the introduced mutations in Core and NS5A do not affect overall protein folding, stability or function (Fig. 4). Taken together, the data show that the association of HCV proteins with LDs is important for the production of infectious viral particles (Fig. 5e).

Our results also indicate that NS proteins around the LDs participate in the assembly of infectious virus particles. In one scenario, NS proteins may indirectly contribute to the different steps of virus production — for example, by establishing the microenvironment around the LDs that is required for infectious virus production. Alternatively, NS proteins around the LDs may directly participate in virus production — for example, as components of the replication complex that provide the RNA genome to the assembling nucleocapsid.

In support of the role of LDs in virus formation, we observed that colocalization of HCV protein with LDs was low in cases of the chimera Jc1, supporting up to 1,000-fold higher infectivity titres compared with JFH1 (ref. 13). In a Jc1-infected cell, only about 20% of LDs demonstrated detectable colocalization with Core, but this value increased to 80% in the case of a Jc1 mutant lacking most of the envelope glycoprotein genes and thus being unable to produce infectious virus particles (data not shown). This inverse correlation between the efficiency of virus production and Core protein accumulation on LDs indicates that rapid assembly and virus release results in the rapid liberation of HCV proteins from the LDs.

Steatosis and abnormal lipid metabolism caused by chronic HCV infection may be linked to enhanced LD formation[14]. In fact, the overproduction of LDs is induced by Core (Supplementary Information, Fig. S3) and HCV also induces membrane rearrangements around LDs (Fig. 3d–f). Our findings suggest that excessive Core-dependent formation of LDs

and membrane rearrangements are required to supply the necessary microenvironment for virus production. NS proteins and HCV RNA seem to be translocated from the ER to the LD-associated membranes. Interestingly, the LD-associated membranes were occasionally found in continuity with ribosome-studded rough ER (Fig. 3e, arrowheads). Thus, at least parts of the LD-associated membranes are likely to be derived from ER membranes. ER marker proteins, however, were not detected in the LD fraction, suggesting that the LD-associated membrane is characteristically distinct from that of ER membranes.

To our knowledge, this is the first report showing that LDs are required for the formation of infectious virus particles. The fact that capsid protein of the hepatitis G virus also localizes to LDs[15] indicates that LDs might be important for the production of other viruses as well. Our findings demonstrate a novel function of LDs, provide an important step towards elucidating the mechanism of HCV virion production and open new avenues for novel antiviral intervention. □

METHODS

Antibodies. The antibodies used for immunoblotting and immunolabelling were specific for Core (#32-1 and RR8); E2 (AP-33 (ref. 23); 3/11, CBH5 and Flag M2 (Sigma-Aldrich, St Louis, MO); NS3 (R212)[17]; NS4A and 4B (PR12); NS5A (NS5ACL1); NS5B (NS5B-6 and JFH1-1)[24]; ADRP (Progen Biotechnik, Heidelberg, Germany); tubulin (Oncogene Research Products, MA, USA); Grp78 (StressGen, Victoria, Canada); PDI (StressGen); and Calnexin-NT (StressGen). Antibodies specific for Core (#32-1 and RR8), NS3 (R212) and NS4AB (PR12) were gifts from Dr Kohara (The Tokyo Metropolitan Institute of Medical Science, Japan). Anti-E2 antibody (AP-33) was provided by Dr Patel (MRC Virology Unit, UK). Anti-NS5B (NS5B-6) antibody was kindly provided by Dr Fukuya (Osaka University, Japan). Rabbit polyclonal antibodies specific for NS5A were raised against a bacterially expressed GST–NS5A (1–406 aa) fusion protein. In the case of the HCV chimeras Con1/C3 and H77/C3, immunofluorescence analyses were performed by using the following antibodies: Core (C7/50)[5], a JFH1 NS3-specific rabbit polyclonal antiserum; NS4B (#86)[25]; and NS5A (Austral Biologicals, San Ramon, CA).

Indirect immunofluorescence analysis. Indirect immunofluorescence analysis was performed essentially as described previously[17], with slight modifications. Cells transfected with JFH1 RNA were seeded onto a collagen-coated Labtech II 8-well chamber (Nunc, NY, USA). The coating with collagen was performed using rat-tail collagen type I (BD Bioscience, Palo Alto, CA) according to manufacturer's instructions. Three days after seeding, the cells were washed twice with phosphate-buffered saline (PBS; 137 mM NaCl, 2.7 mM KCl, 4.3 mM Na_2HPO_4 and 1.4 mM KH_2PO_4) and fixed with fixation solution (4% paraformaldehyde and 0.15 M sodium cacodylate at pH 7.4) for 15 min at room temperature. After washing with PBS, the cells were permeabilized with 0.05% Triton X-100 in PBS for 15 min at room temperature. For the precise localization of the proteins, the cells were permeabilized with 50 μg ml^{-1} of digitonin in PBS for 5 min at room temperature[26]. After incubating the cells with blocking solution (10% fetal bovine serum and 5% bovine serum albumin (BSA) in PBS) for 30 min, the cells were incubated with the primary antibodies. The fluorescent secondary antibodies were Alexa 568- or Alexa 647-conjugated anti-mouse or anti-rabbit IgG antibodies (Invitrogen, Carlsbad, CA). Nuclei were labelled with 4',6-diamidino-2-phenylindole (DAPI). LDs were visualized with BODIPY 493/503 (Invitrogen). Analyses of JFH1 were performed on a Leica SP2 confocal microscope (Leica, Heidelberg, Germany). Analysis of the Con1/C3 and the H77/C3 chimeras was performed in the same way, except that imaging was performed on a Nikon C1 confocal microscope (Nikon, Tokyo, Japan).

Electron microscopy. For conventional electron microscopy, cells cultured in plastic Petri dishes were processed *in situ*. The cells were fixed in 2.5% glutaraldehyde and 0.1 M sodium phosphate (pH 7.4), and then in OsO_4 and 0.1 M sodium phosphate (pH 7.4). The cells were then dehydrated in a graded ethanol series and embedded in an epoxy resin. Ultrathin sections were cut perpendicular to the base of the dish. For immuno-electron microscopy, cells were detached from the dish with a cell scraper after fixation in 4% paraformaldehyde, 0.1% glutaraldehyde and 0.1 M sodium phosphate (pH 7.4) for 24 h, and washed in 0.1 M lysine, 0.1 M sodium phosphate (pH 7.4) and 0.15 M sodium chloride. After dehydrating the cells in a graded series of cold ethanol, they were embedded in Lowicryl K4M at −20 °C. Ultrathin sections were labelled with primary antibodies and colloidal gold particles (15 nm) conjugated to anti-mouse IgG or anti-rabbit IgG antibodies. For double labelling, colloidal gold particles with different diameters (10 nm and 15 nm) conjugated to anti-mouse IgG or anti-rabbit antibodies were used. Samples were observed after staining with uranyl acetate and lead citrate with a JEM 1010 electron microscope at the accelerating voltage of 80 kV. Anti-Core (#32-1 and RR88), anti-NS5A (NS5ACL1) and anti-E2 (Flag M2) antibodies were used.

Preparation of the lipid droplets. Cells at a confluency of ~80% on a dish with a diameter of 14 cm were scraped in PBS. The cells were pelleted by centrifugation at 1,500 rpm. The pellet was resuspended in 500 μl of hypotonic buffer (50 mM HEPES, 1 mM EDTA and 2 mM $MgCl_2$ at pH 7.4) supplemented with protease inhibitors (Roche Diagnostics, Basel, Switzerland) and was incubated for 10 min at 4 °C. The suspension was homogenized with 30 strokes of a glass Dounce homogenizer using a tight-fitting pestle. Then, 50 μl of 10× sucrose buffer (0.2 M HEPES, 1.2 M KoAc, 40 mM $Mg(oAc)_2$ and 50 mM DTT at pH 7.4) was added to the homogenate. The nuclei were removed by centrifugation at 2,000 rpm for 10 min at 4 °C. The supernatant was collected and centrifuged at 16,000 *g* for 10 min at 4 °C. The supernatant (S16) was mixed with an equal volume of 1.04 M sucrose in isotonic buffer (50 mM HEPES, 100 mM KCl, 2 mM $MgCl_2$ and protease inhibitors). The solution was set at the bottom of 2.2-ml ultracentrifuge tube (Hitachi Koki, Tokyo, Japan). One milliliter of isotonic buffer was loaded onto the sucrose mixture. The tube was centrifuged at 100,000 *g* in an S55S rotor (Hitachi Koki) for 30 min at 4 °C. After the centrifugation, the LD fraction on the top of the gradient solution was recovered in isotonic buffer. The suspension was mixed with 1.04 M sucrose and centrifuged again at 100,000 *g*, as described above, to eliminate possible contamination with other organelles. The collected LD fraction was used for western blotting or the HCV RNA synthesis assay.

HCV RNA synthesis assay. An assay of HCV RNA synthesis using digitonin-permeabilized cells was performed as described previously[17]. For RNA synthesis assays using the LD fraction, the LD fraction collected by sucrose-gradient sedimentation was suspended in buffer B, which contained 2 mM manganese (II) chloride, 1 mg ml^{-1} acetylated BSA (Nacalai Tesque, Kyoto, Japan), 5 mM phosphocreatine (Sigma), 20 units/ml creatine phosphokinase (Sigma), 50 μg ml^{-1} actinomycin D, 500 μM ATP, 500 μM CTP, 500 μM GTP (Roche Diagnostics) and 1.85 MBq of [α-^{32}P] UTP (GE Healthcare, Little Chalfont, UK), and incubated at 27 °C for 4 h. The reaction products were analysed by gel electrophoresis followed by autoradiography.

Note: Supplementary Information is available on the Nature Cell Biology website.

ACKNOWLEDGEMENTS

We thank T. Fujimoto and Y. Ohsaki at Nagoya University for helpful discussions and technical assistance. Y.M. is a recipient of a JSPS fellowship. K.S. is supported by Grants-in-Aid for cancer research and for the second-term comprehensive 10-year strategy for cancer control from the Ministry of Health, Labour and Welfare, as well as by a Grant-in-Aid for Scientific Research on Priority Areas "Integrative Research Toward the Conquest of Cancer" from the Ministry of Education, Culture, Sports, Science and Technology of Japan. T.W. is also supported, in part, by a Grant-in-Aid for Scientific Research from the Japan Society for the Promotion of Science; and by the Research on Health Sciences Focusing on Drug Innovation from the Japan Health Sciences Foundation. R.B. is supported by the Sonderforschungsbereich 638 (Teilprojekt A5) and the Deutsche Forschungsgemeinschaft (BA1505/2-1). M.Z. and R.B. thank the Nikon Imaging Center at the University of Heidelberg for providing access to their confocal fluorescence microscopes and Ulrike Engel for the excellent support.

AUTHOR CONTRIBUTIONS

Y.M. and K.S. planned experiments and analyses. Y.M. was responsible for experiments for Figs 1, 2, 3a–c, 4a–e and 5b. K.A., N.U., electron microscopy; T.H., Fig. 1e; M.Z., R.B., Fig. S2e; and K.S. and K.W., Fig. 4f–g. T.W. provided JFH1 strain. Y.M. and K.S. wrote the manuscript. All authors discussed the results and commented on the manuscript.

COMPETING FINANCIAL INTERESTS
The authors declare no competing financial interests.

Published online at http://www.nature.com/naturecellbiology/
Reprints and permissions information is available online at http://npg.nature.com/reprintsandpermissions/

1. Martin, S. & Parton, R. G. Lipid droplets: a unified view of a dynamic organelle. *Nature Rev. Mol. Cell Biol.* **7**, 373–378 (2006).
2. Blanchette-Mackie, E. J. *et al.* Perilipin is located on the surface layer of intracellular lipid droplets in adipocytes. *J. Lipid Res.* **36**, 1211–1226 (1995).
3. Vock, R. *et al.* Design of the oxygen and substrate pathways. VI. structural basis of intracellular substrate supply to mitochondria in muscle cells. *J. Exp. Biol.* **199**, 1689–1697 (1996).
4. Liang, T. J. *et al.* Viral pathogenesis of hepatocellular carcinoma in the United States. *Hepatology* **18**, 1326–1333 (1993).
5. Moradpour, D., Englert, C., Wakita, T. & Wands, J. R. Characterization of cell lines allowing tightly regulated expression of hepatitis C virus core protein. *Virology* **222**, 51–63 (1996).
6. Deleersnyder, V. *et al.* Formation of native hepatitis C virus glycoprotein complexes. *J. Virol.* **71**, 697–704 (1997).
7. Kato, N. *et al.* Molecular cloning of the human hepatitis C virus genome from Japanese patients with non-A, non-B hepatitis. *Proc. Natl Acad. Sci. USA* **87**, 9524–9528 (1990).
8. Hijikata, M. & Shimotohno, K. [Mechanisms of hepatitis C viral polyprotein processing]. *Uirusu* **43**, 293–298 (1993).
9. Dubuisson, J., Penin, F. & Moradpour, D. Interaction of hepatitis C virus proteins with host cell membranes and lipids. *Trends Cell Biol.* **12**, 517–523 (2002).
10. Wakita, T. *et al.* Production of infectious hepatitis C virus in tissue culture from a cloned viral genome. *Nature Med.* **11**, 791–796 (2005).
11. Lindenbach, B. D. *et al.* Complete replication of hepatitis C virus in cell culture. *Science* **309**, 623–626 (2005).
12. Zhong, J. *et al.* Robust hepatitis C virus infection in vitro. *Proc. Natl Acad. Sci. USA* **102**, 9294–9299 (2005).
13. Pietschmann, T. *et al.* Construction and characterization of infectious intragenotypic and intergenotypic hepatitis C virus chimeras. *Proc. Natl Acad. Sci. USA* **103**, 7408–7413 (2006).
14. Moriya, K. *et al.* Hepatitis C virus core protein induces hepatic steatosis in transgenic mice. *J. Gen. Virol.* **78**, 1527–1531 (1997).
15. Hope, R. G., Murphy, D. J. & McLauchlan, J. The domains required to direct core proteins of hepatitis C virus and GB virus-B to lipid droplets share common features with plant oleosin proteins. *J. Biol. Chem.* **277**, 4261–4270 (2002).
16. Egger, D. *et al.* Expression of hepatitis C virus proteins induces distinct membrane alterations including a candidate viral replication complex. *J. Virol.* **76**, 5974–5984 (2002).
17. Miyanari, Y. *et al.* Hepatitis C virus non-structural proteins in the probable membranous compartment function in viral genome replication. *J. Biol. Chem.* **278**, 50301–50308 (2003).
18. Quinkert, D., Bartenschlager, R. & Lohmann, V. Quantitative analysis of the hepatitis C virus replication complex. *J. Virol.* **79**, 13594–13605 (2005).
19. Tauchi-Sato, K., Ozeki, S., Houjou, T., Taguchi, R. & Fujimoto, T. The surface of lipid droplets is a phospholipid monolayer with a unique fatty acid composition. *J. Biol. Chem.* **277**, 44507–44512 (2002).
20. Londos, C., Brasaemle, D. L., Schultz, C. J., Segrest, J. P. & Kimmel, A. R. Perilipins, ADRP, and other proteins that associate with intracellular neutral lipid droplets in animal cells. *Semin. Cell Dev. Biol.* **10**, 51–58 (1999).
21. Blight, K. J., McKeating, J. A. & Rice, C. M. Highly permissive cell lines for subgenomic and genomic hepatitis C virus RNA replication. *J. Virol.* **76**, 13001–13014 (2002).
22. Klein, K. C., Dellos, S. R. & Lingappa, J. R. Identification of residues in the hepatitis C virus core protein that are critical for capsid assembly in a cell-free system. *J. Virol.* **79**, 6814–6826 (2005).
23. Owsianka, A. *et al.* Monoclonal antibody AP33 defines a broadly neutralizing epitope on the hepatitis C virus E2 envelope glycoprotein. *J Virol* **79**, 11095–11104 (2005).
24. Ishii, N. *et al.* Diverse effects of cyclosporine on hepatitis C virus strain replication. *J. Virol.* **80**, 4510–4520 (2006).
25. Lohmann, V., Korner, F., Herian, U. & Bartenschlager, R. Biochemical properties of hepatitis C virus NS5B RNA-dependent RNA polymerase and identification of amino acid sequence motifs essential for enzymatic activity. *J Virol* **71**, 8416–8428 (1997).
26. Ohsaki, Y., Maeda, T. & Fujimoto, T. Fixation and permeabilization protocol is critical for the immunolabeling of lipid droplet proteins. *Histochem. Cell Biol.* **124**, 445–452 (2005).

nature
cell biology

Supplementary Figures and legends

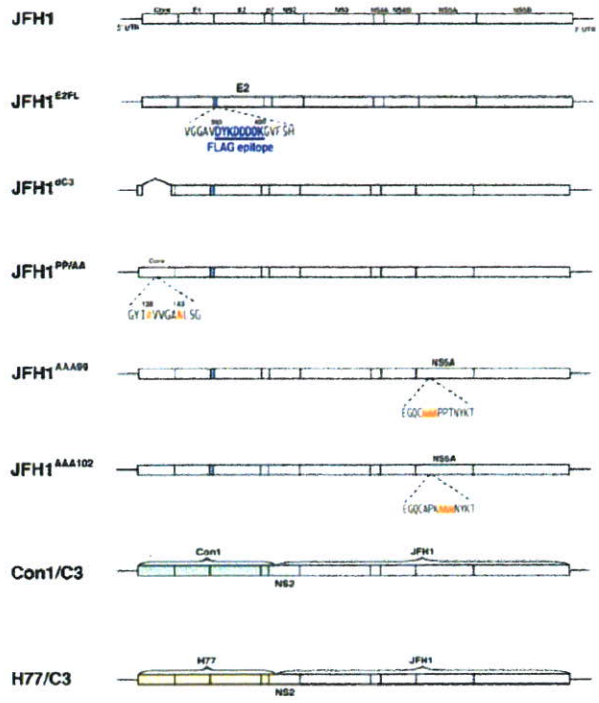

Supplementary Fig. 1

Schematic structures of HCV genomes and mutants used in this study

In JFH1^{E2FL}, the amino acid residues at positions 393 to 400 in the hyper variable region 1 of E2 were converted to a Flag epitope: DYKDDDDK. The JFH1^{E2FL} genome was used to generate other mutant variants of JFH1. In these cases the Flag epitope is marked with a blue vertical line. JFH1^{dC3} carried a deletion in the Core gene that eliminated the 17th to the 163rd amino-acid residue of Core. JFH1$^{PP/AA}$ is a mutant of JFH1^{E2FL} carrying alanine substitutions for proline residues at amino-acid positions 138 and 143 in Core. JFH1^{AAA99} and JFH1^{AAA102} contained mutated NS5A genes carrying triple-alanine substitutions for the APK sequence at amino acid positions 99 to 101 and the PPT sequence at amino acid positions 102 to 104, respectively. Constructs Con1/C3 and H77/C3 are chimeras in which the region from Core to the N-terminal domain of NS2 of JFH1 was replaced by the analogous region of the genotype 1b isolate Con1 or by the genotype 1a isolate H77[6].

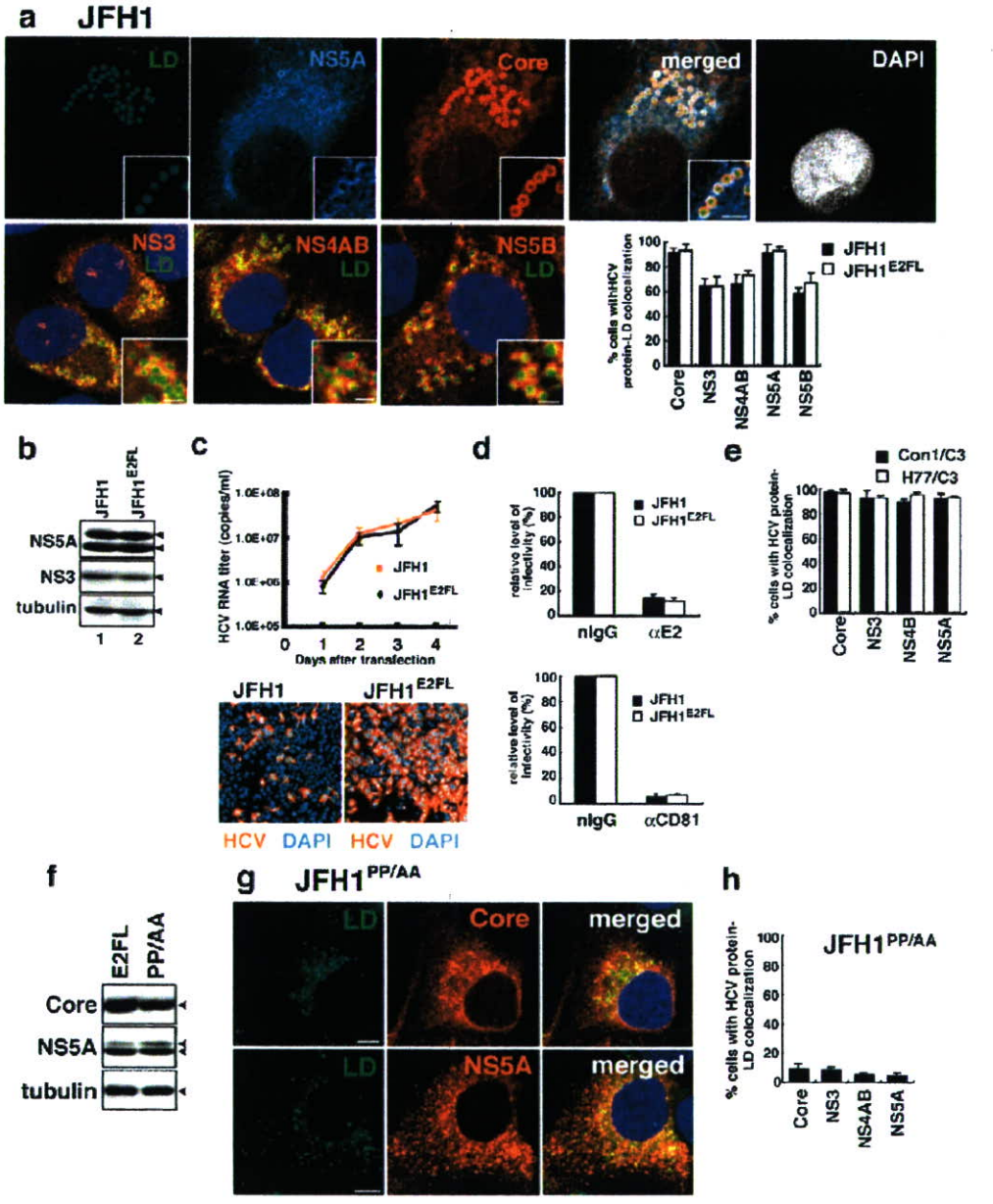

Supplementary Fig. S2 Kunitata Shimotohno
NCB-S11732B

Supplementary Fig. 2 Characterization of mutant JFH1s

(a) JFH1-replicating cells were stained with indicated antibodies, BODYPI 493/503 and

DAPI. Scale bars = 2 μm. Percentages of JFH1- and JFH1^{E2FL}-replicating cells with overlapping signals for LDs and HCV proteins (n > 200). (b) HCV proteins in JFH1 and JFH1^{E2FL} replicating cells were analyzed by western blotting with indicated antibodies. (c) Efficiency of virus production and infectivity of JFH1 and JFH1^{E2FL} viruses were analyzed as described in Fig. 4. (n = 3) (d) Inhibition of HCV infection by anti-E2 antibody and anti-CD81 antibody. JFH1 and JFH1^{E2FL} virus were pre-incubated with normal IgG (nIgG) or anti-E2 antibody for 1 hr at 4°C and were subsequently used to inoculate Huh-7.5 cells (upper panel). Huh-7.5 cells were pre-incubated with normal IgG (nIgG) or anti-CD81 antibody for 1 hr at 37°C before inoculation with JFH1 or JFH1^{E2FL} viruses (lower panel) (n = 3). No obvious difference with respect to the subcellular localization of viral proteins (a), efficiency of viral replication (b), virus production (c), and pathway of virus entry (d) were observed between JFH1^{E2FL} and JFH1 (e) Con1/C3 or H77/C3 replicating cells were stained for HCV antigens (Core or NS3 or NS4B or NS5A) and LDs. The graphs show the percentage of Con1/C3 (black) or H77/C3 (white) positive cells in which HCV protein signals overlapped with LD signals. The overlapping signals were detected by using the ImageJ RG2B software package (n > 200). (f) Whole-cell extracts of JFH1^{E2FL} (E2FL) and JFH1$^{PP/AA}$ (PP/AA) replicon-bearing cells were analyzed by Western blot with indicated antibodies. Both Core^{Wt} and Core$^{PP/AA}$ had an apparent molecular weight of about 21 kDa, indicating that Core$^{PP/AA}$ was efficiently processed. The expression level of Core$^{PP/AA}$, however, was slightly lower than that of Core^{Wt}. (g) Analysis of the subcellular localization of Core and NS5A in cells bearing the JFH1$^{PP/AA}$ mutant. Cells were labeled to detect LDs (green), Core (red), NS5A (red) and nuclei DAPI (blue). Scale bars = 10μm. (h) The percentages of JFH1$^{PP/AA}$ replicon-bearing cells positive for overlapping signals of LDs and HCV proteins are indicated (n > 200).

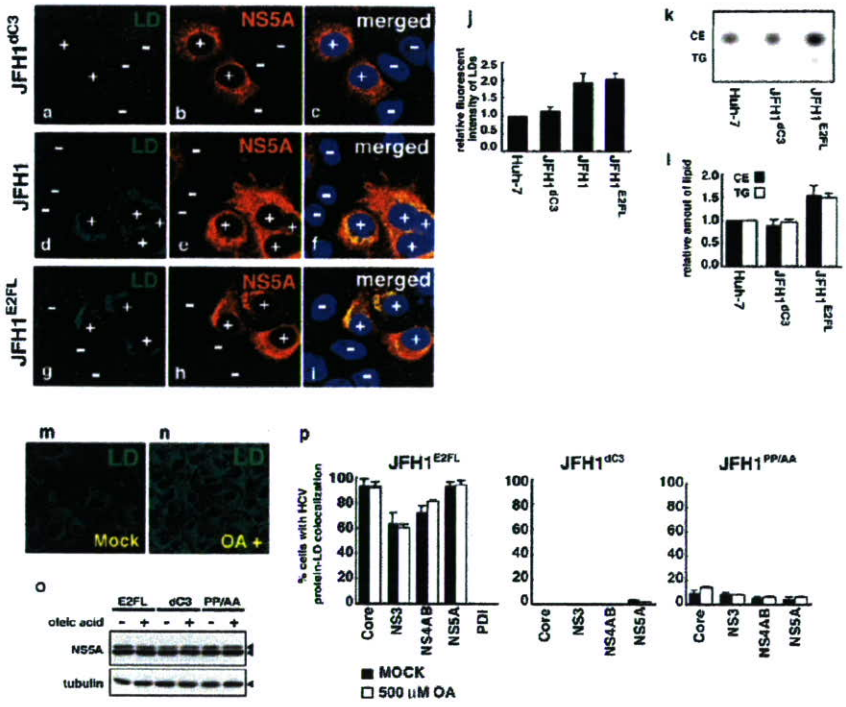

Supplementary Fig. S3 Kunitata Shimotohno
NCB-S11732B

Supplementary Fig. 3

Enhanced formation of LDs in JFH1- and JFH1^{E2FL}-replicating cells

Cells transfected with JFH1^{dC3} (a-c), JFH1 (d-f), and JFH1^{E2FL} RNA (g-i) were stained with BODIPY493/503 (green), DAPI (blue), and anti-NS5A antibody (red). + and – indicate HCV-positive and HCV-negative cells, respectively. Fluorescence intensities of LDs in Huh-7 cells, JFH1^{dC3}-, JFH1-, and JFH1^{E2FL}-replicating cells were measured by confocal microscopy. The results are represented as relative fluorescence intensity of LDs (j). (k and l) Lipid fraction extracted from Huh-7 cells, JFH1^{dC3}-, and JFH1^{E2FL}-replicating cells was analyzed by thin-layer chromatography. Each lane was loaded with lipid corresponding to an equal amount of protein. Cholesterol ester (CE) and triglyceride (TG) are indicated (k). The relative intensity of CE and TG in panel k is shown in l (n = 3). (m-p) JFH1^{E2FL} replicon-bearing cells were treated with 500 μM oleic acid for 24 hrs and were labeled with BODIPY493/503 (m and n). Cells transfected with JFH1^{E2FL} (E2FL), JFH^{dC3} (dC3), or JFH$^{PP/AA}$ (PP/AA) RNA were treated with or without oleic acid. (o) The HCV protein level as represented by the level of NS5A was analyzed by western blot. (p) The percentages of cells positive for overlapping signals for LDs and the HCV proteins or PDI are indicated. The data was obtained in the presence (500 μM) or absence (MOCK) of oleic acid in the culture medium (n > 200).

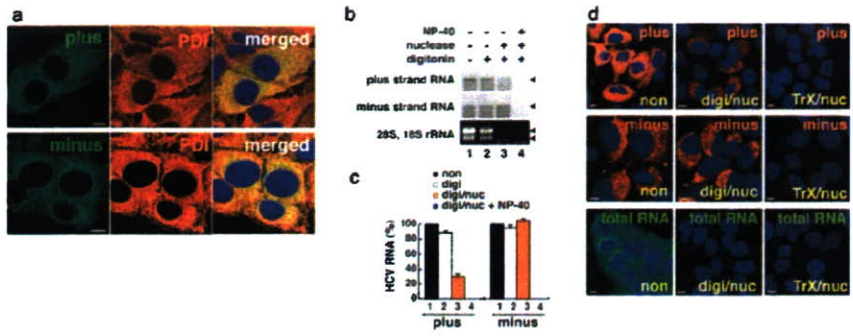

Supplementary Fig. S4 Kunitata Shimotohno
NCB-S11732B

Supplementary Fig. 4

Subcellular localizations of plus- and minus-strand HCV RNA

(a) JFH1^{E2FL} replicating cells were analyzed by *in situ* hybridization to detect plus- and minus-strand HCV RNA (green). The cells were also labeled with anti-PDI antibodies (red) and DAPI (blue). Scale bars = 10 μm. (b, c) Relative amounts of plus- and minus-strand HCV RNAs. JFH1^{E2FL}-expressing cells were permeabilized with digitonin. The cells were treated with nuclease in the presence or absence of NP-40. Then, total RNA was analyzed by Northern blots with strand-specific HCV RNA probes. 28S and 18S ribosomal RNA was stained with ethidium bromide (b). The signals were quantified and plotted in c (n = 3). The amounts of plus- and minus-strand RNA were similar before and after digitonin treatment (lanes 1 and 2). The level of plus-strand RNA, however, was reduced by approximately 70% after nuclease treatment, whereas the level of minus-strand RNA remained constant (lanes 2 and 3). Nuclease treatment in the presence of NP-40 used to lyse the membranes caused both plus- and minus-strand HCV RNA to disappear (lane 4). This result suggests that ~30% and ~100% of plus- and minus-strand HCV RNA, respectively, are located in the replication complexes. (d) Localization of nuclease-resistant JFH1^{E2FL} RNA was analyzed by *in situ* hybridization. Digitonin-permeabilized cells were treated with nuclease in the presence (TrX/nuc) or absence (digi/nuc) of Triton X-100. Total RNA was visualized with SYTO RNAselect. "non" indicates cells without digitonin and nuclease treatment. Using the nuclease-resistant HCV RNA as a marker of replication complexes, we examined the localization of the replication complexes. Both plus- and minus-strand HCV RNA were detected in the perinuclear region even after the nuclease treatment. As expected, these RNAs were no longer detectable after nuclease treatment in the presence of Triton X-100. The intensity of the plus-strand RNA signal decreased after nuclease treatment (compare upper left and middle panels). However, the intensity of the minus-strand RNA signal remained unchanged after the treatment. These results correlated with the data obtained by Northern blotting analysis. For this reason, the percentages of cells with overlapping signals for LDs and plus- or minus-strand HCV RNA (Fig. 2c) were measured after lysis of cells with digitonin and nuclease treatment. Scale bars = 10 μm.

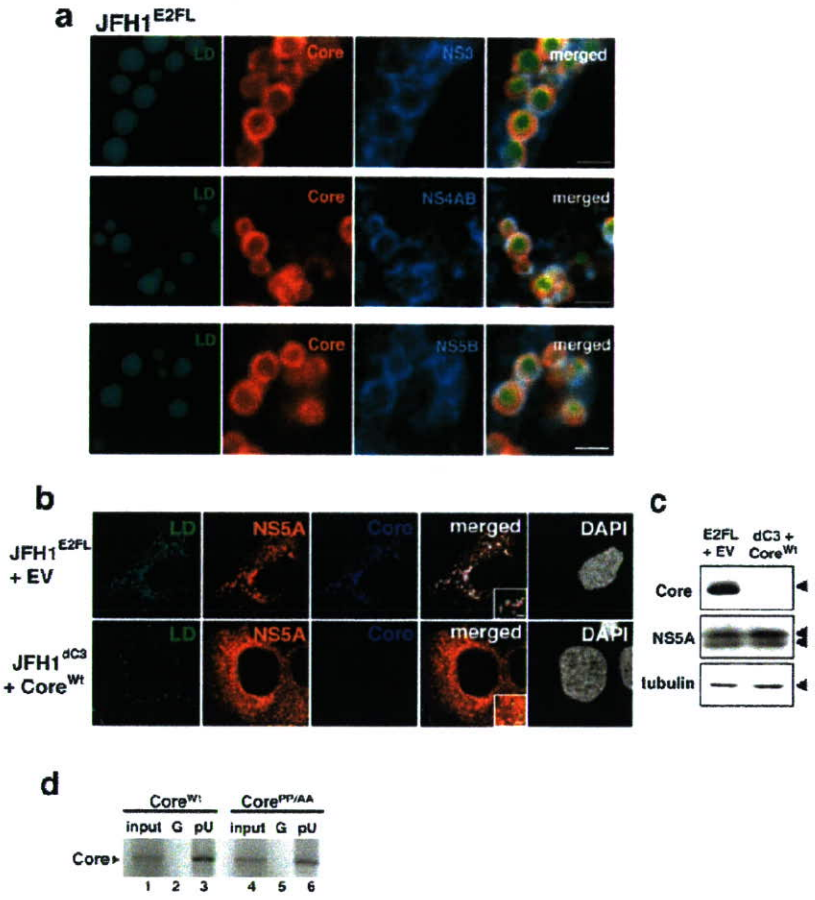

Supplementary Fig. S5 Kunitata Shimotohno NCB-S11732B

Supplementary Fig. 5

Subcellular localization of HCV proteins in JFH1^{E2FL}-replicating cells and cells inoculated with rescued viruses, and RNA binding nature of Core.

(a) JFH1^{E2FL}-replicating cells were labeled to detect LDs (green), Core (red), NS3 (cyan), NS4AB (cyan), and NS5B (cyan). Scale bars = 2 μm **(b)** The subcellular localizations of NS5A and Core in Huh-7.5 cells infected with viruses released from JFH1^{E2FL} replicon-bearings cells co-transfected with pcDNA3 (upper panels) and from JFH1^{dC3} replicon-bearing cells co-transfected with pcDNA3-Core^{Wt} (lower panels). Cells were labeled with DAPI (white), BODIPY 493/503 (green), anti-Core (blue), and anti-NS5A (red) antibodies. The insets are high magnifications of the corresponding panel. (c) HCV proteins from these infected cells were analyzed by western blotting. (d) An RNA-protein binding precipitation assay was performed with *in vitro*-translated and ^{35}S-radiolabeled Core^{Wt} (lane 1-3) and Core$^{PP/AA}$ (lane 4-6). The resulting precipitates were analyzed by SDS-PAGE and detected by autoradiography. "G" and "pU" mark samples obtained using protein G Sepharose and poly-U Sepharose as the resin, respectively. "input" indicates 1/20 of the amount of translated product used in this assay.

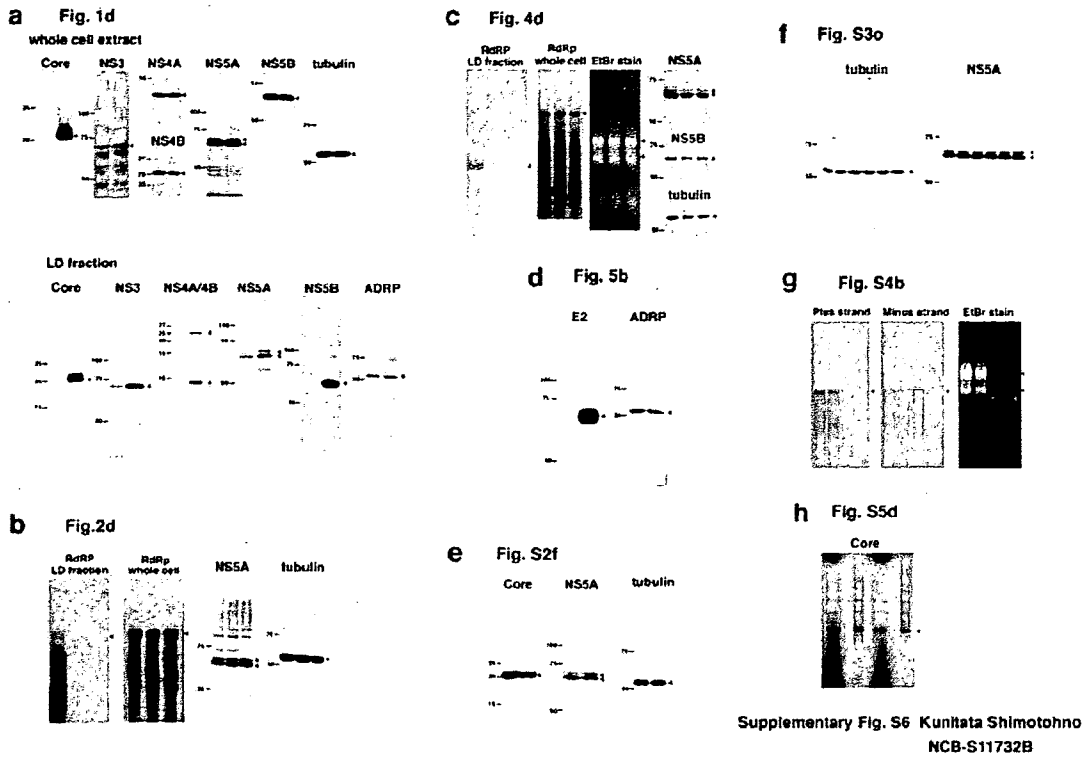

Supplementary Fig. 6

Full scan of key gel images depicted in the individual figures.

Full scans of (a) immunoblot detection of whole cell extract and LD fraction from JFH1^{E2FL}- and JFH1^{dC3}-replicating cells shown in Fig. 1d, (b) RNA synthesis assay and immunoblot detection of JFH1^{E2FL}-, JFH1^{dC3}-, and JFH1$^{PP/AA}$-replicating cells shown in Fig. 2d, (c) RNA synthesis assay and immunoblot detection of JFH1^{E2FL}-, JFH1^{AAA99}-, and JFH1^{AAA102}-replicating cells shown in Fig. 4d, (d) immunoblot detection of LD fraction from JFH1^{E2FL}- and JFH1^{dC3}-replicating cells shown in Fig. 5b, (e) immunoblot detection of JFH1^{E2FL}- and JFH1$^{PP/AA}$-replicating cells shown in Fig. S2f, (f) immunoblot detection of JFH1^{E2FL}-replicating cells shown in Fig. S3o, (g) Northern Blotting analysis of JFH1^{E2FL}-replicating cells shown in Fig. S4b, and (h) RNA-protein binding precipitation assay shown in Fig. S5d. Size of molecular weight markers (kDa) is indicated at the left side of western blot gel images. *In vitro* transcribed HCV RNA was used as a size marker for RNA gel electrophoresis (b, c, and g).

plasmid name	primer sequences (5' to 3')	template for PCR	restriction enzyme	original plasmid
pcDNA3-Core ^{WT}	AGACCCAAGCTTCACCATGAGCACAAATCCTAAACC	pJFH1	HindIII	pcDNA3
	AATGGAATTCTCAAGCAGAGACCGGAACGGTGATGC		EcoRI	
pcDNA3-TME2	AGACCCAAGCTTGACCATGGGTGACTGGGGGGTCATGTTC	pJFH1	HindIII	pcDNA3
	AATGCAATTCTCATCCTTCGGCCTCCCCCAACAAC		EcoRI	
pcDNA3-NS3	AGACCCAAGCTTGACCATGGGTCCCATCACTGCTTATGCC	pJFH1	HindIII	pcDNA3
	AATGGAATTCTCAGGTCATGACCTCAAGGTCAGC		EcoRI	
pcDNA3-NS4B	AGACCCAAGCTTGACCATGGGCTCTAGGGCGGCTCTCATCC	pJFH1	HindIII	pcDNA3
	AATGGAATTCTCAGCATGGGATGGGGCAGTCCTC		EcoRI	
pcDNA3-NS5B	CTCGGATCCACCATGTCCATGTCATACTCCTGGACC	pJFH1	BamHI	pcDNA3
	AATGGAATTCCTACCGAGCGGGGAGTAGGAAGAGG		EcoRI	
pcDNA3-Core $^{PP/AA}$	CATGGGGTACATCGCCGTCGTAGGCGCCGCCTTAGTGGCG	pJFH1 $^{PP/AA}$	HindIII	pcDNA3
	CGCCACTAAGCGCGGCGCCTACGACGGCGATGTACCCCATG		EcoRI	
pJFH1 ^{E2FL}	GATTACAAGGATGACGACGATAAGGGCGTGTTCAGCCATGGCCC	pJFH1	BsiWI	pJFH1
	CTTATCGTCGTCATCCTTGTAATCAACAGGCCCTCCAACGGTGG		NotI	
	GGGACATGATGATGAACTGG			
	GTAATGTCAAACACCACACC			
pJFH1 ^{WT}	GAAAAACCAAAAGAAACAGCAACTATGCAACAGGGAACCTACC	pJFH1 ^{E2FL}	EcoRI	pJFH1 ^{E2FL}
	GTTGGTGTTTCTTTTGGTTTTTC		BsiWI	
	CGCACATGATGATGAACTGC			
	GTAATGTCAAACACCACACC			
pJFH1 $^{PP/AA}$	CATGGGGTACATCGCCGTCGTAGGCGCCGCCGCTTAGTGGCG	pJFH1 ^{E2FL}	EcoRI	pJFH1 ^{E2FL}
	CGCCACTAAGCGGCGGCGCCTACGACGGCGATGTACCCCATG		BsiWI	
	CGCACATGATGATGAACTGC			
	GTAATGTCAAACACCACACC			
pJFH1 ^{E2FL} dBamHI	TACTGCCTGCCATCCTGTCTGC	pJFH1 ^{E2FL}	NsiI	pJFH1 ^{E2FL}
	GGAGACAGGATGCCAGGCAGTA		RsrII	
	CTATTACCAATGAGGTCACC			
	CAACAATTTACAGGTCAGCC			
pJFH1 ^{AA339}	GGCCAGTGCCGCGGCGGCACCGCCCACG	pJFH1 ^{E2FL}	BamHI	pJFH1 ^{E2FL} dBamHI
	CGTCGGGCGTCCCGCCGCCACTCGCC		RsrII	
	TGGATGAACAGGCTTATTGC			
	GGTTGAAGCTCTACCTGATC			
pJFH1 ^{AA337}	GCGCCGAAAGCCGCCGCGAACTACAAG	pJFH1 ^{E2FL}	BamHI	pJFH1 ^{E2FL} dBamHI
	CTTGTAGTTCCGCGCCGCTTTCGGCGC		RsrII	
	TGGATGAACAGGCTTATTGC			
	GGTTGAAGCTCTACCTGATC			

Supplementary Table

A list of the plasmids used in this work. The sets of primers used to amplify the target genes, the template plasmids used in the PCRs, the restriction sites, and plasmids into which the amplified DNA fragments were inserted are shown.

Supplementary Materials and Methods

Cell culture

The human hepatoma cell lines Huh-7 and Huh-7.5[1] were grown in Dulbecco's modified Eagle's medium (DMEM; Invitrogen, CA, USA) supplemented with 10% fetal bovine serum (FBS), 100 U/ml nonessential amino acids (Invitrogen), and 100 μg/ml penicillin and streptomycin sulfate (Invitrogen). Huh-7.5 cells were obtained from Dr. C. Rice. (Rockefeller University, USA)

Plasmid construction

All plasmids were generated by insertion of PCR-amplified fragments into expression plasmids. The plasmids, the primer sequences, templates for the PCRs, and the restriction enzyme sites used to construct the plasmids are listed in Supplementary Table 1.

DNA and RNA transfection

Transfection of HCV RNA was performed as previously described[2]. DNA transfection was performed using Lipofectamine 2000 (Invitrogen) according to the manufacturer's instructions.

Northern blotting

Northern blot analysis was performed as described previously[3] with strand specific RNA probes.

RT-PCR analysis

Quantitative real-time RT-PCR analysis of the HCV RNA titer was performed as described previously[4].

ELISA for the detection of Core

Core in the culture medium was quantified with an ELISA according to the manufacturer's protocol (HCV antigen ELISA test, Ortho-Clinical Diagnostics).

Thin-layer chromatography

Lipid samples extracted from cells were dissolved in chloroform methanol and were